A multi-photon fluorescent probe based on quinoline groups for highly selective and sensitive detection of lipid droplets

Sijing Zhang[¶a], Zhenghui Yang[¶b], Minghao Li[¶a], Qiong zhang[a*], Xiaohe Tian[b], Dandan Li[c], Shengli Li[a], Jieying Wu[b], Yupeng Tian[a*].

[a.] *Department of Chemistry, Key Laboratory of Functional Inorganic Material Chemistry of Anhui Province, Anhui University, Hefei 230601, P. R. China.*

[b.] *School of Life Science, Anhui University, Hefei 230039, P. R. China.*

[c.] *Institutes of Physics Science and Information Technology, Anhui University, Hefei 230039, P. R. China.*

¶ These authors contributed equally to this work.
E-mail address: *zhangqiong.314@163.com* *yptian@ahu.edu.cn*

Materials and apparatus

All chemicals were purchased as reagent grade and used without further purification. The solvents were dried and distilled according to standard procedures. IR spectra (4000 - 400 cm^{-1}), as KBr pellets, were recorded on a Nicolet FT-IR 870 SX spectrophotometer. ^{1}H-NMR spectra were performed on a Bruker 400 Hz Ultra shield spectrometer and reported as parts per million (ppm) from TMS (δ), ^{13}C-NMR spectra were obtained on a Bruker Advance 100 MHz NMR spectrometer. UV-*vis* absorption spectra were recorded on a UV-265 spectrophotometer. Fluorescence measurements were carried out on a Hitachi F-7000 fluorescence spectrophotometer.

Experimental Section

1.1 Synthesis and characterization

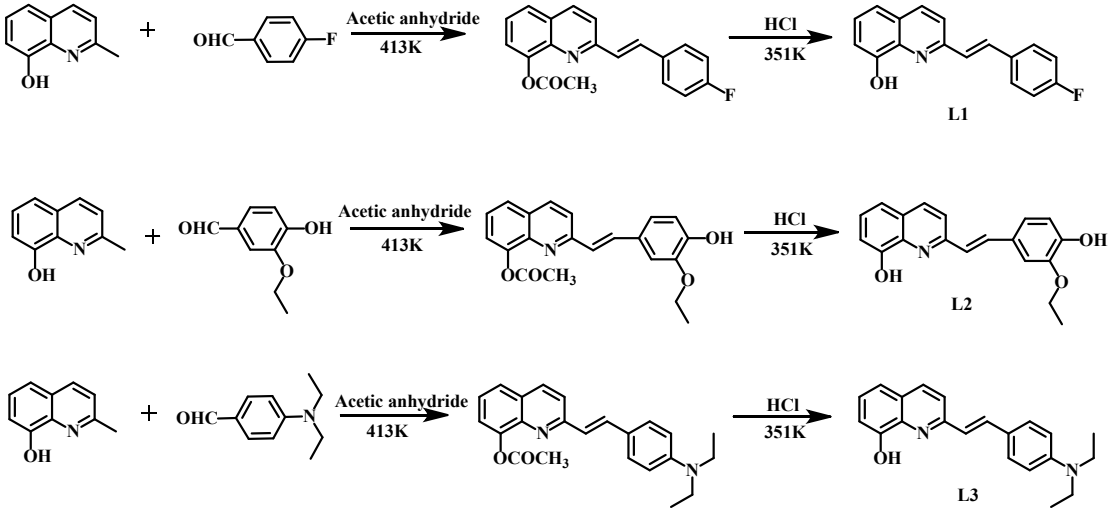

Scheme S1. Synthetic routes of **L1**, **L2** and **L3**.

The 8-Hydroxyquinaldine 50 mmol (7.95 g) and $\mathbf{M_{1\text{-}3}}$ (p-Fluoro benzaldehyde, ethyl vanillin, 4-Diethylaminobenzaldehyde) 62.5 mmol (7.75 g, 10.37 g, 11.06 g) were dissolved with 40 mL acetic anhydride, the mixture were reacted for 40 h at 413 K in N_2 atmosphere. And the reaction mixture was converted from colourless to green. After reaction finished, cooling to room temperature, dropping the reaction solution into water slowly, the intermediate object was got buy filtration. Then the intermediate object 20 mmol (6.14 g, 6.98 g, 7.2 g) were dissolved with 50 ml ethanol, and 3 ml HCl were added dropwise, the mixture were reacted for 2 h at 351 K. The solid was filtered when cooling to room temperature. All crystals were recrystallized from ethanol.

L1: Ethanol recrystallization was obtained as colorless powder. Yield 8.6 g (45.1%)。M.p.=133 ~135 °C. ESI-MS: calc: 265.10, found: 266.10 $[M+H]^{+}$. ^{1}H NMR (400 MHz, DMSO-d6) δ: 9.56

(s, 1H), 8.30 (d, J = 8.6 Hz, 1H), 8.13 (d, J = 16.2 Hz, 1H), 7.77 (dd, J = 8.3, 5.1 Hz, 3H), 7.38 (ddd, J = 19.9, 17.5, 12.7 Hz, 3H), 7.30 (t, J = 8.8 Hz, 2H), 7.10 (d, J = 6.9 Hz, 1H). ^{13}C NMR (100 MHz, CD_3COCD_3) δ:164.20, 161.65, 153.68, 152.76, 138.22, 136.67, 133.22, 129.18, 127.55, 127.27, 120.98, 117.55, 115.86, 115.42, 110.27. FT-IR (KBr, cm^{-1}): 3402 (m), 3057 (m), 1797 (w), 1632 (s), 1593 (s), 1508 (s), 986 (s), 971 (s), 872 (s), 839 (s), 760 (s), 715 (s), 589 (s).

L2: Ethanol recrystallization was obtained as yellow powder. Yield 9.4 g (47.3%)。M.p.=136 ~ 138 °C. ESI-MS: calc: 307.12, found: 308.12 $[M+H]^+$. ^{1}H NMR (400 MHz, CD_3COCD_3) δ: 8.12 (d, J = 8.6 Hz, 1H), 7.85 (d, J = 16.2 Hz, 1H), 7.61 (d, J = 8.6 Hz, 1H), 7.23 (dt, J = 26.8, 12.1 Hz, 4H), 7.06 (d, J = 8.0 Hz, 1H), 6.97 (d, J = 6.4 Hz, 1H), 6.76 (d, J = 8.1 Hz, 1H), 4.08 (q, J = 7.0 Hz, 2H), 1.41 (m, 3H). ^{13}C NMR (100 MHz, CD_3COCD_3) δ: 154.59, 152.40, 148.02, 146.92, 138.12, 136.33, 135.04, 128.61, 127.60, 126.88, 125.05, 121.53, 120.80, 117.63, 115.17, 110.91, 110.08, 64.33, 14.18. FT-IR (KBr, cm^{-1}): 3514 (m), 2978 (m), 1927 (m), 1846 (m), 1639 (s), 1562 (s), 1510 (s), 1042 (s), 958 (s), 826 (s), 755 (s), 715 (s), 561(s).

L3: Ethanol recrystallization was obtained as yellow powder. Yield 8.6 g (53.7%)。M.p.=82 ~84 °C. ESI-MS: calc: 318.17, found: 319.17 $[M+H]^+$. ^{1}H NMR (400 MHz, CD_3COCD_3) δ: 8.67 (d, J = 8.6 Hz, 1H), 8.40 (d, J = 16.1 Hz, 1H), 8.18 (d, J = 8.6 Hz, 1H), 8.01 (d, J = 8.8 Hz, 2H), 7.86(m, 2H), 7.65 (d, J = 16.1 Hz, 1H), 7.54 (dd, J = 7.0, 1.7 Hz, 1H), 7.22 (d, J = 8.8 Hz, 2H), 3.92 (q, J = 7.0 Hz, 4H), 1.64 (t, J = 7.0 Hz, 6H). ^{13}C NMR (100 MHz, CD_3COCD_3) δ: 155.01, 152.56, 148.46, 138.26, 136.23, 135.32, 128.99, 127.33, 126.50, 123.67, 122.23, 120.72, 117.55, 111.55, 109.96, 44.03, 12.10. FT-IR (KBr, cm^{-1}): 3352 (s), 3025 (s), 2971 (s), 1911 (m), 958 (s), 884 (m), 862 (s), 690 (s), 532 (s).

1.2 Crystallography

The single crystals of **L1**, **L2** and **L3**, suitable for X-ray diffraction analysis, were obtained from methanol solution at room temperature. The relevant crystal data and structural parameters were summarized in **Table S1**. The selected bond distances and angles were listed in **Table S2**.

The X-ray diffraction measurements were accomplished on a Bruker SMART CCD area detector using graphite monochromated Mo-Kα radiation (λ = 0.71069 Å) at 298(2) K. Intensity data were collected in the variable ω-scan mode. The structures were solved by direct methods and difference Fourier transformations. The nonhydrogen atoms were refined anisotropically and

hydrogen atoms were introduced geometrically. Calculations were performed with SHELXTL-97 program package.

1.3 Computational details

The ground states for each molecule were calculated using the density functional theory level with the B3LYP functional employing a 6-31G* basis set. The absorption energies were investigated by time-dependent density functional theory (TD-DFT). All calculations were performed by the use of the Gaussian 03 suite of programs.

1.4 1.3 Two-photon absorption cross-section

Two-photon absorption cross-sections of CM2P, CM4P were obtained by the two-photon excited fluorescence (TPEF) method at femtosecond laser piles and a Ti: sapphire system (680-1080 nm, 80 MHz, 140 fs) as the light source. Effective two-photon absorption cross-section (σΦ) values were determined by the following equation:

$$\boldsymbol{\sigma\Phi} = \sigma_{ref}\Phi_{ref}\frac{C_{ref}}{C}\frac{n_{ref}}{n}\frac{F}{F_{ref}}$$

The subscripts ref stands for the Fluorescein. Φ is the quantum yield, n is the refractive index, F is the integrated area under the corrected emission spectrum, c is the concentration of the solution in mol·L-1. The σref value of reference was taken from the literature[1].

1.5 Three-photon excitation fluorescence (3PEF) measurements

All the samples were contained in 1cm-optical length quartz liquid cell and Rhodamin 6G as the standard sample for intensity comparison. Spectrometer: Ocean Optics QE65 Pro (300-2500 nm). Laser: Coherent Astrella+TOPAS Prime (1100-1700) nm, 1 kHz, 120 fs. All the results provided here are the 10 times average results[2-3].

Theory:

$$\sigma_{3s} = \frac{c_R \times n_s \times f_s \times Q_R}{c_s \times n_R \times f_R \times Q_S} \times \sigma_{3R}$$

where the subscripts “s” and “r” represent sample and reference (here, Rhodamine 6G in ethanol solution at a concentration of 1.0×10^{-3} mol/L was used as reference), respectively. F is the overall fluorescence collection efficiency intensity of the fluorescence signal collected by the fiber spectra meter. Q, n and c are the quantum yield of the fluorescence, the refractive index of solvent, and the concentration of the solution, respectively.

1.6 Cell imaging

HeLa cells were seeded in 24-well glass bottom plate at a density of 2 × 104 cells per well and grown for 96 h. For live cell imaging, cell cultures were incubated with the complexes (10% PBS: 90% cell media) at concentration 4 μM and maintained at 310 K in an atmosphere of 5% CO2 and 95% air for incubation times ranging for 30 min. The cells were then washed with PBS (3 × 1 ml per well) and 1 mL of PBS was added to each well. The cells were imaged using confocal laser scanning microscopy using oil immersion lenses.

1.7 STED imaging

STED nanoscopy experiments were performed under a Leica DMi8 confocal microscope equipped with a Leica TCS SP8 STED-ONE unit, the compound was excited under an STED laser, and the emission signals were collected using HyD reflected light detectors. Specimen living cells were prepared using a method similar to normal confocal microscopy described previously. The STED micrographs were further processed using “deconvolution wizard” function using Huygens Professional software (version: 16.05) under authorized license.

1.8 Cytotoxicity test

The effects of L1, L2 and L3 on viability of cells were carried out using the methylthiazolyldiphenyl-tetrazolium bromide (MTT) assay. Hela cells were trypsinized and plated to 70 % confluence in 96 well plates 24 h before treatment. Prior to the compounds’ treatment, the DMEM was removed and replaced with fresh DMEM, and aliquots of the L1, L2 and L3 stock solutions were diluted to obtain the final concentrations of 2, 4, 6, 8, 10 μM. The treated cells were then incubated at 310 K in 5% CO2 for 24 h. Subsequently, the cells were treated with 5 mg/mL MTT (10 μL per well) and incubated for an additional 4 h (310 K, 5% CO2). Then,

DMEM was removed, the formazan crystals were dissolved in DMSO (100 μL per well), and the absorbance at 490 nm using a microplate reader (SpectraMax Paradigm). The absorbance measured for an untreated cell population under the same experimental conditions was used as the reference point to establish 100% cell viability. Duplicated experiments have been tested.

1.9 Preparation of liposome and O/W emulsions

Liposome: Phosphatidyl choline (100 mg) was dissolved in 20 mL chloroform. After the solvent was evaporated under reduced pressure at 310 K, then 50 mL PBS buffer solution was added, the mixed solution was stirred with magnetic stirring or ultrasonic oscillation at room temperature for 2 h.

O/W emulsions： Glycerol trioleat (63.9 mg) was added to 50 mL PBS buffer solution containing 0.0025 mM hexadecyl trimethyl ammonium bromide as emulsifier to stabilize the O/W emulsion， the mixed solution was stirred with magnetic stirring or ultrasonic oscillation at room temperature for 6 h.

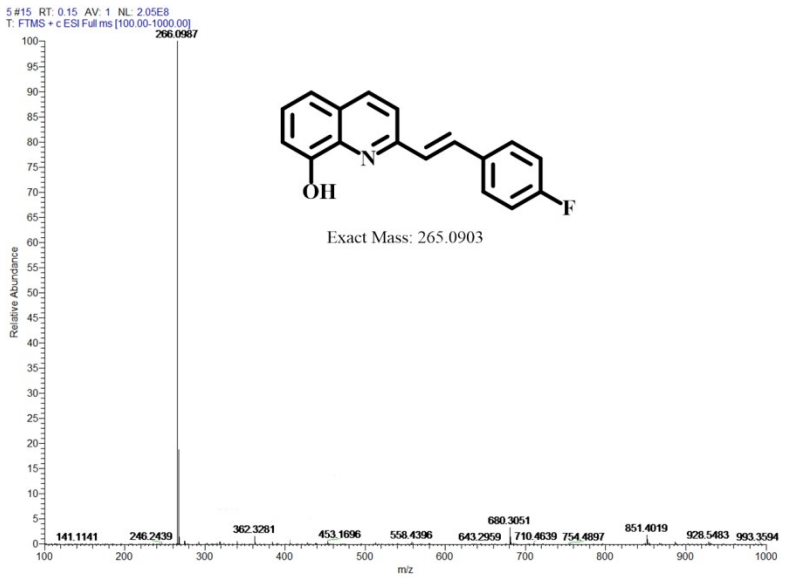

Figure. S1. MS Spectra of **L1**.

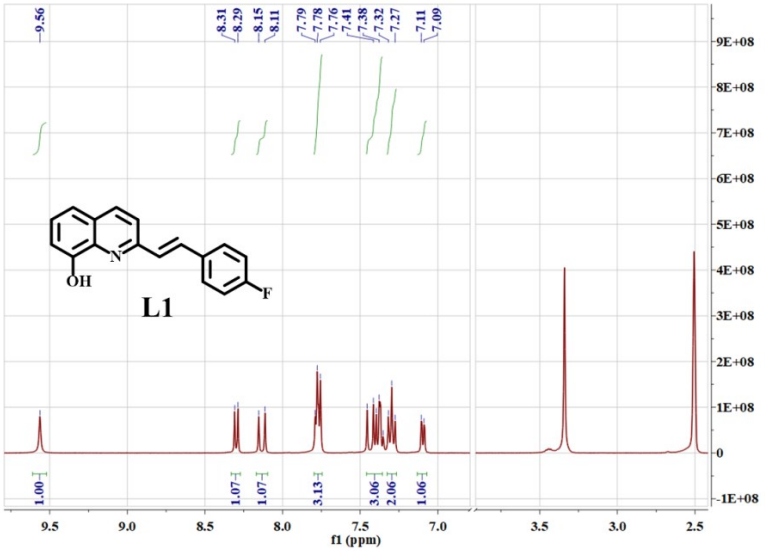

Figure. S2. ^{1}H NMR spectrum of **L1**.

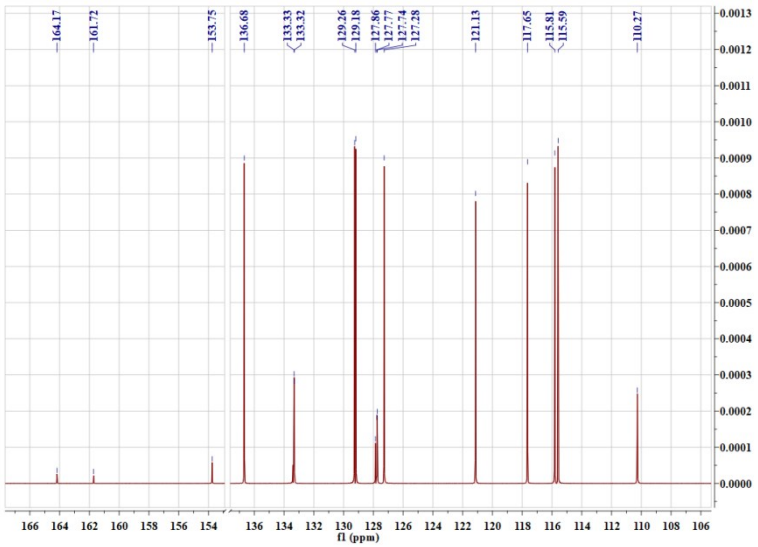

Figure. S3. ^{13}C NMR spectrum of **L1**.

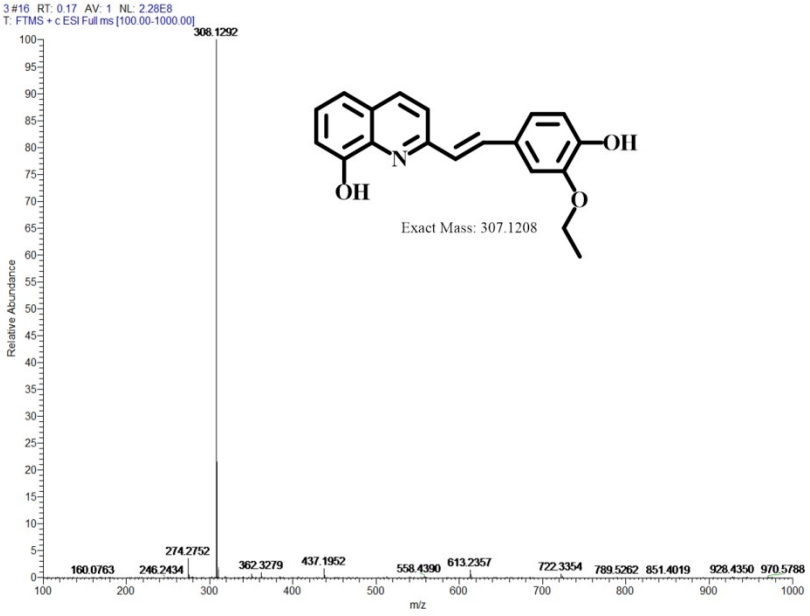

Figure. S4. MS Spectra of **L2**.

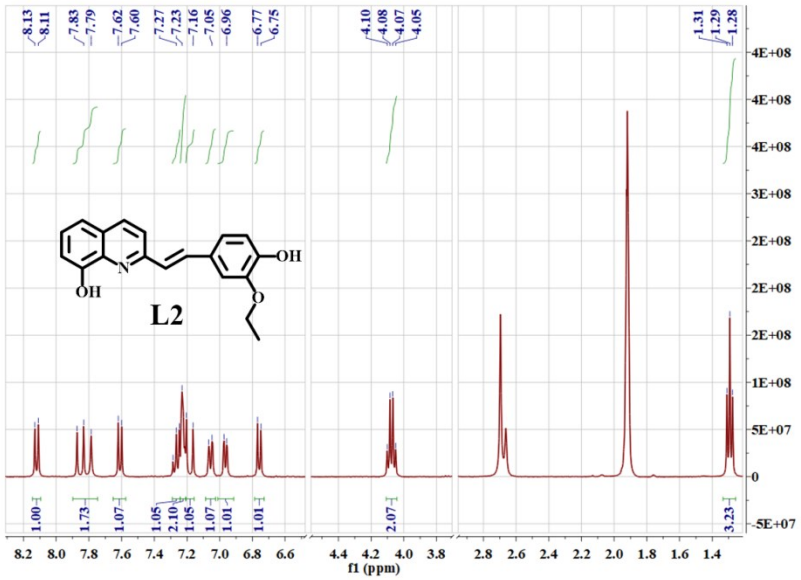

Figure. S5. ^{1}H NMR spectrum of **L2**.

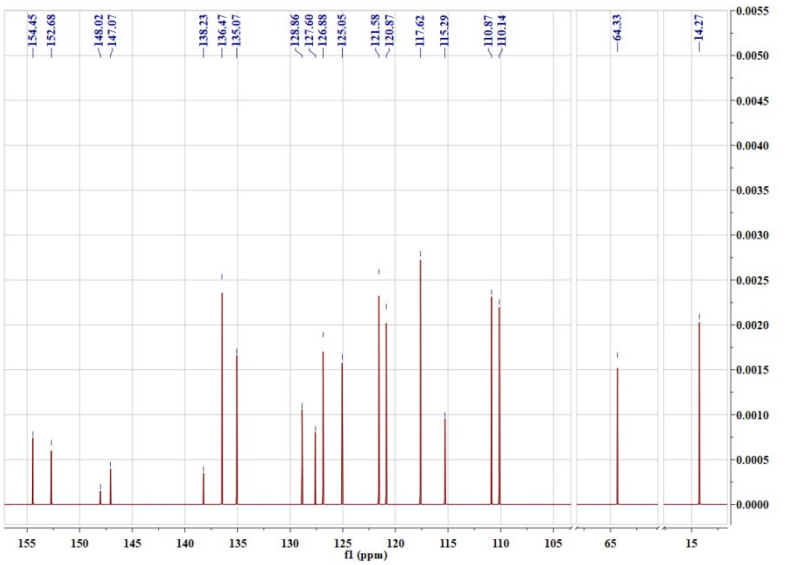

Figure. S6. ^{13}C NMR spectrum of **L2**

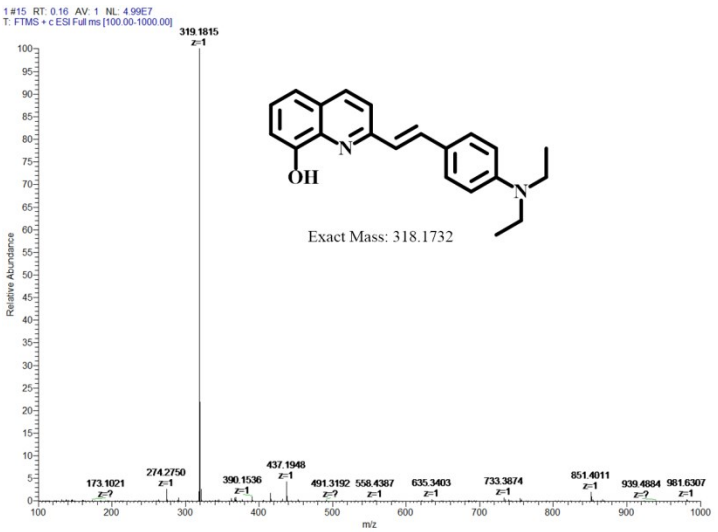

Figure. S7. MS Spectra of **L3**.

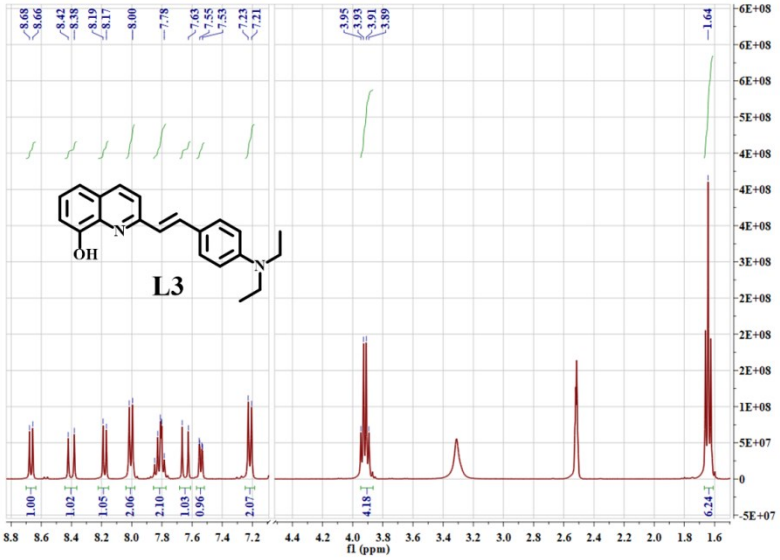

Figure. S8. ^{1}H NMR spectrum of **L3**.

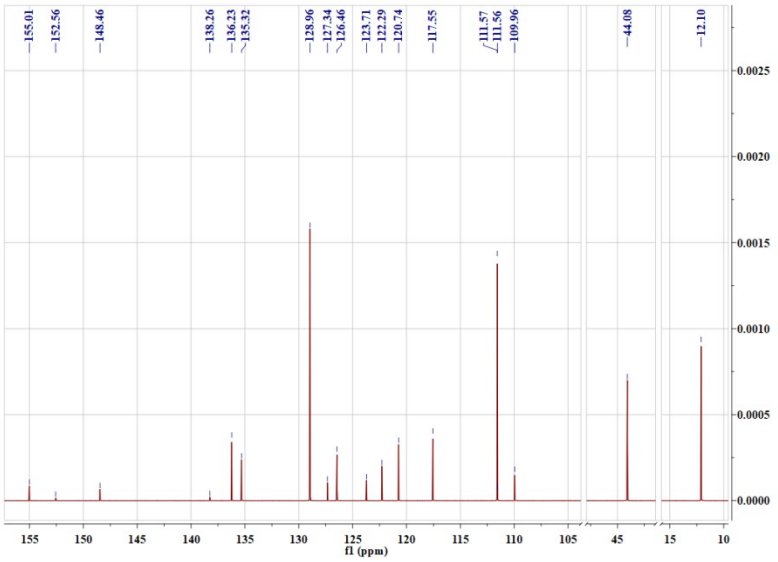

Figure. S9. ^{13}C NMR spectrum of **L3**

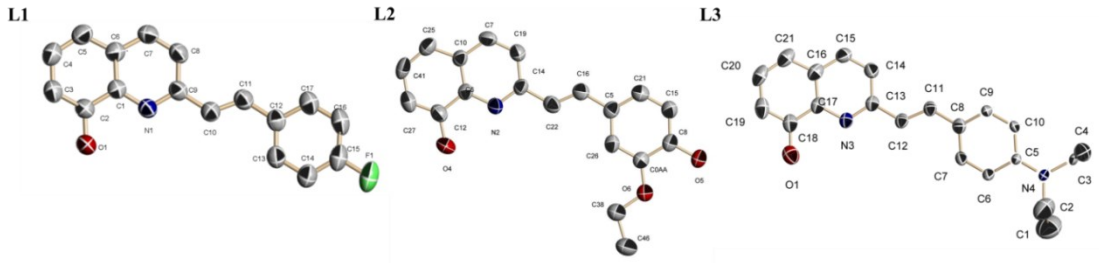

Figure. S10. The ORTEP structure of **L1**, **L2** and **L3** with atomic labeling scheme (with 50% thermal ellipsoidprobability); all hydrogen atoms are omitted for clarity.

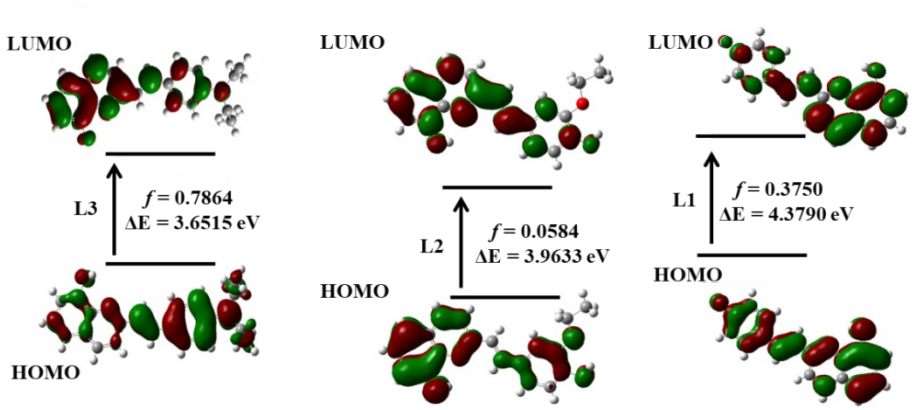

Figure. S11. Molecular orbital energy diagrams for **L1**, **L2** and **L3**.

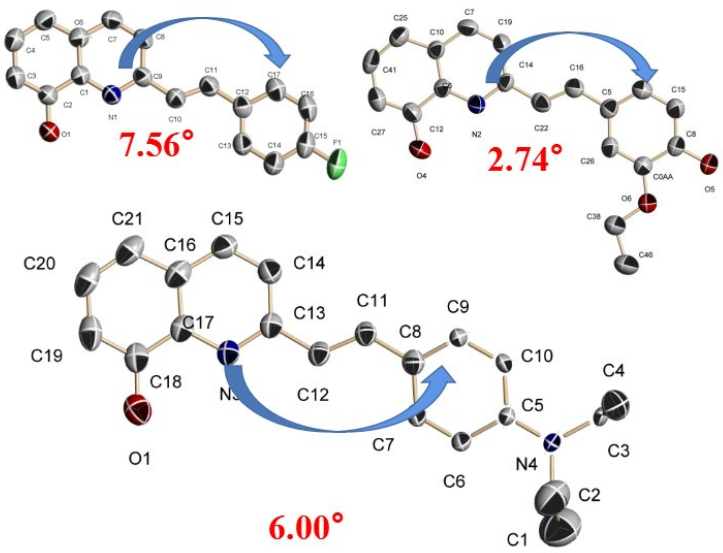

Figure. S12. Molecular dihedral angle diagram of **L1, L2** and **L3.**

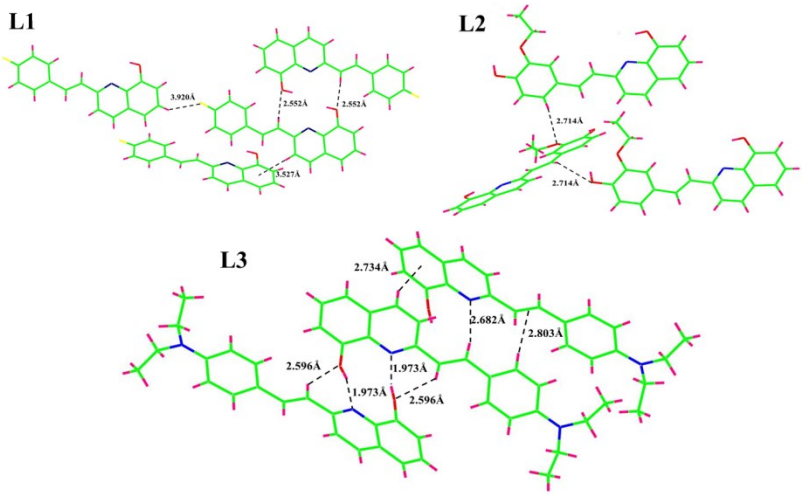

Figure S13. The intermolecular hydrogen bond diagram of **L1**, **L2** and **L3**.

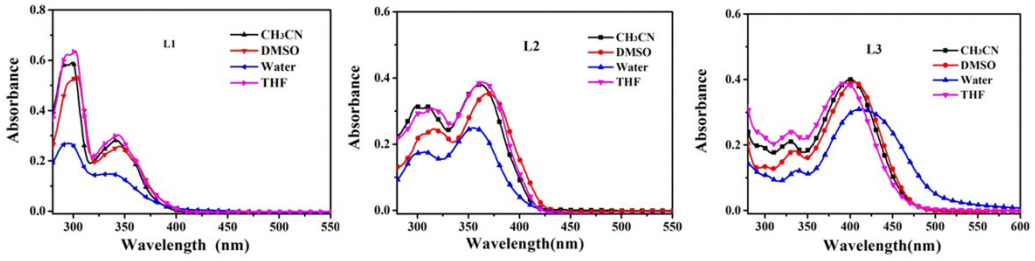

Figure. S14. Linear absorption spectra of **L1**, **L2** and **L3** in different solvents (c = 0.01 mM).

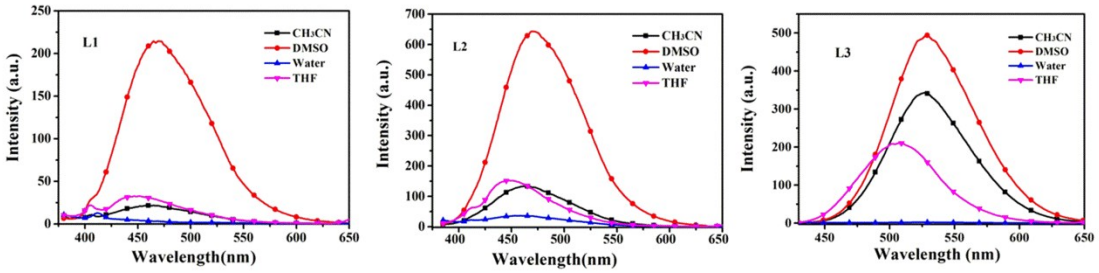

Figure. S15. Single-photon excited fluorescence spectra of **L1**, **L2** and **L3** in different solvents (c = 0.01 mM).

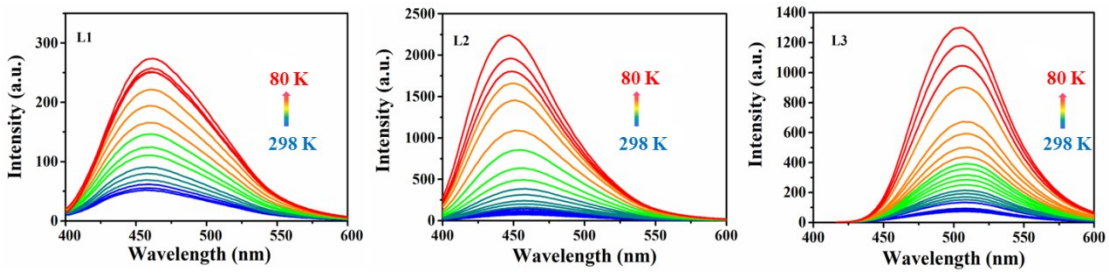

Figure. S16. Single-photon fluorescence spectra of **L1** ~ **L3** at different temperatures (c = 0.01 mM).

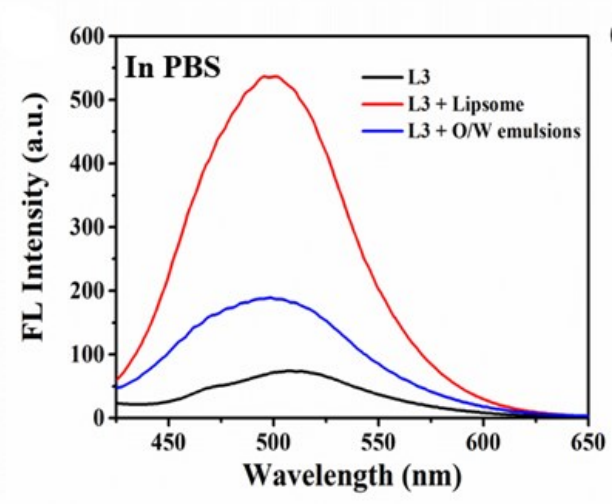

Figure. S17. Single-photon fluorescence intensity of **L3** with liposome and O/W emulsions (λ_{ex} = 405 nm)

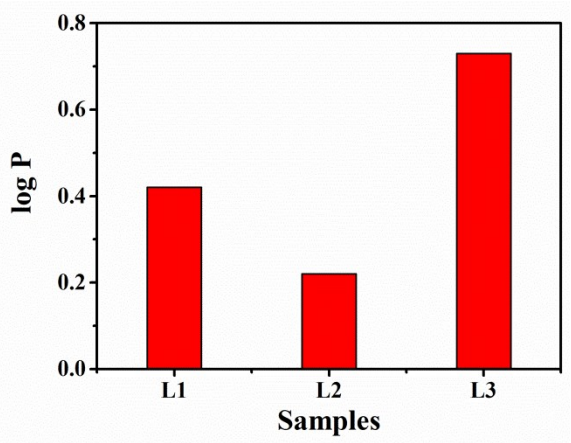

Figure. S18. Octanol value of compounds.

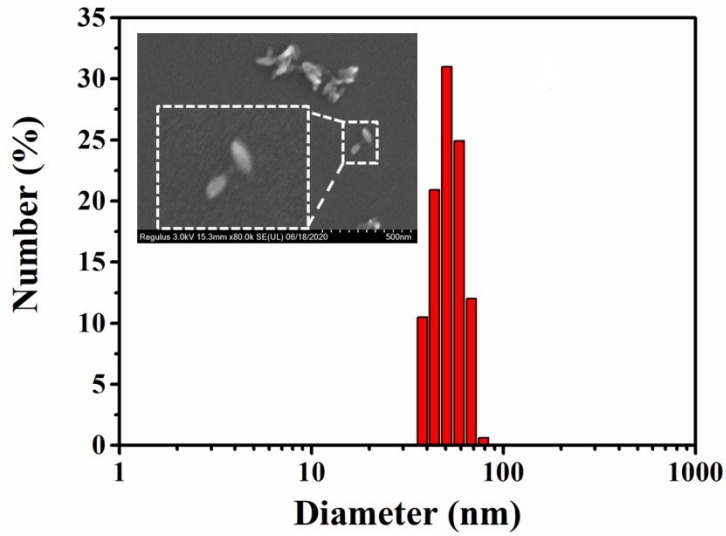

Figure. S19. Size distribution and SEM images (insets) of **L3**.

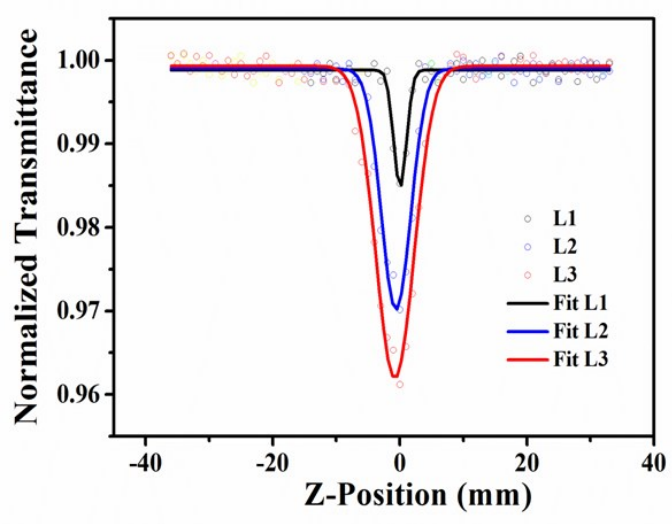

Figure. S20. Theoretical curves of a representative open-aperture Z-scan data of **L1** ~ **L3** in DMSO (λ_{ex} = 840 nm, c = 1 mM).

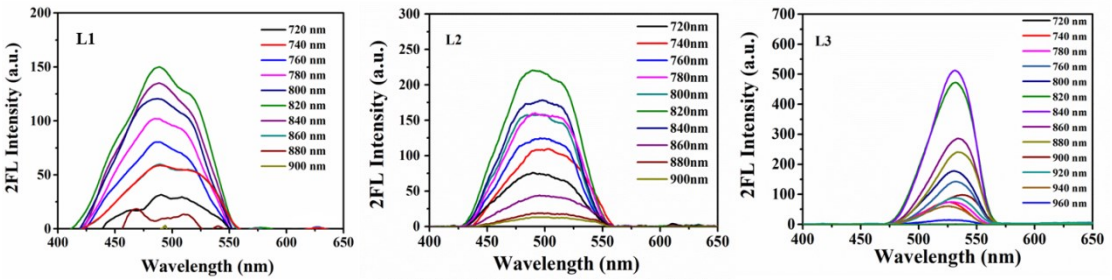

Figure. S21. Two-photon fluorescence spectra of **L1**~**L3** in DMSO with excitation wavelength around 720 ~ 980 nm (c = 1 mM).

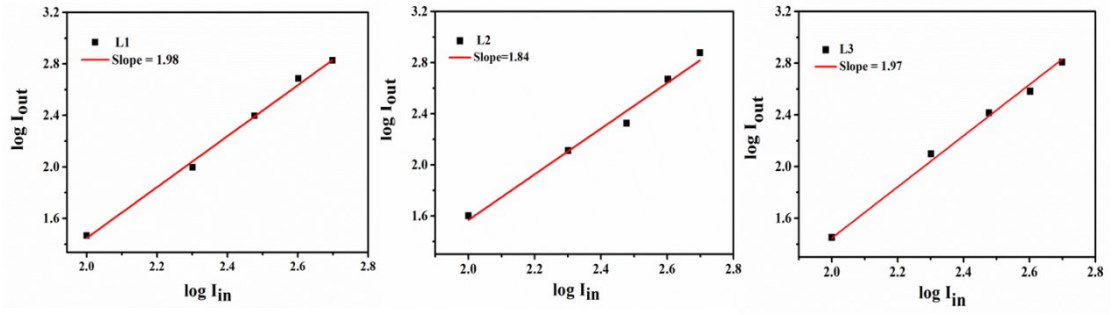

Figure. S22. Two-photon verification of **L1**~**L3** in DMSO.

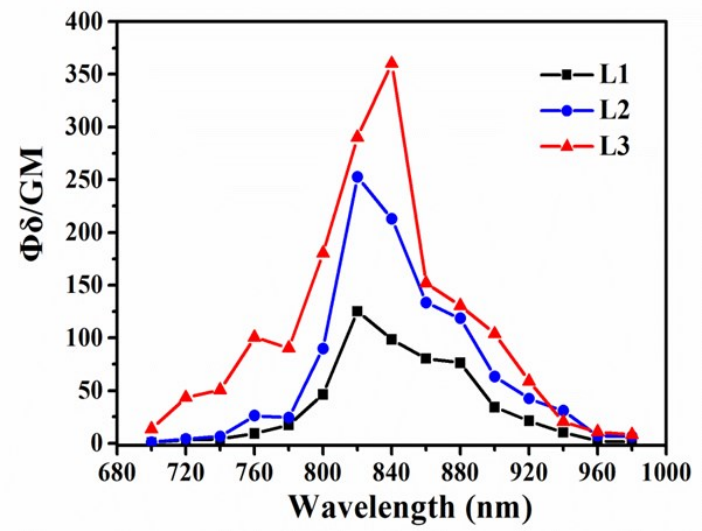

Figure. S23. Two-photon absorption cross section of **L1**~**L3** in DMSO with excitation wavelength around 720 ~ 980 nm (c = 1 mM).

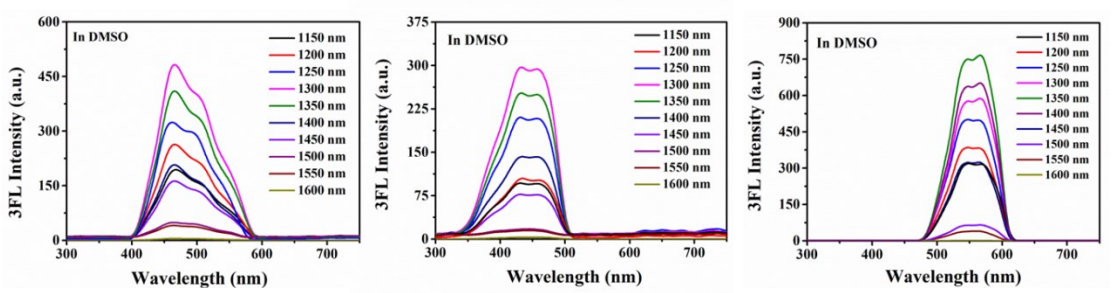

Figure. S24. Three-photon fluorescence spectra of **L1~L3** in DMSO with excitation wavelength around 1150 ~ 1600 nm (c = 1 mM).

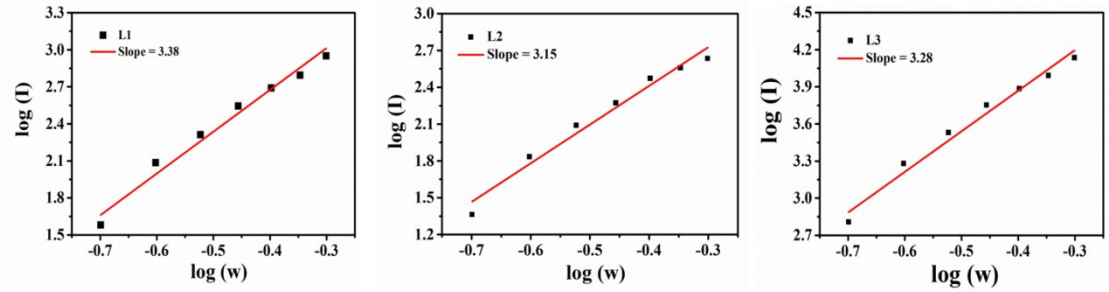

Figure. S25. Three-photon verification of **L1~L3** in DMSO.

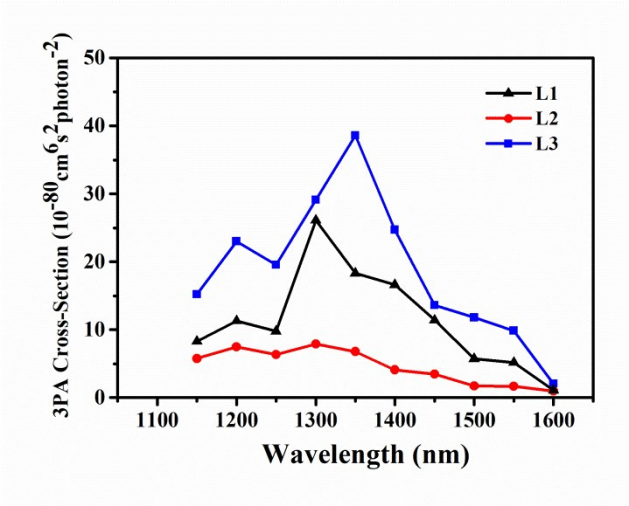

Figure. S26. Three-photon absorption cross section of **L1 ~ L3** in DMSO with excitation wavelength around 1150 ~ 1600 nm (c = 1 mM).

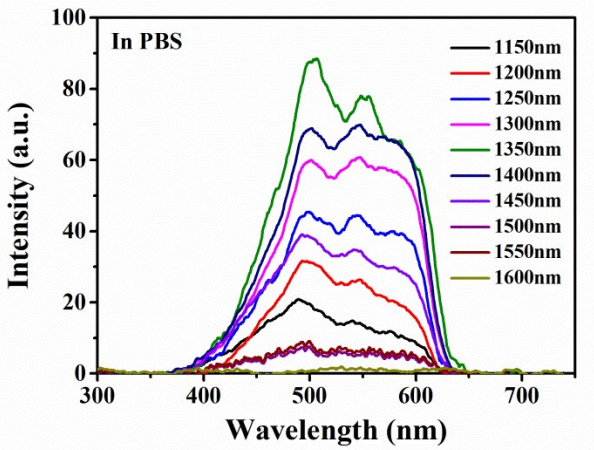

Figure. S27. Three-photon fluorescence spectra of **L3** in PBS with excitation wavelength around 1150 ~ 1600 nm (c = 1 mM).

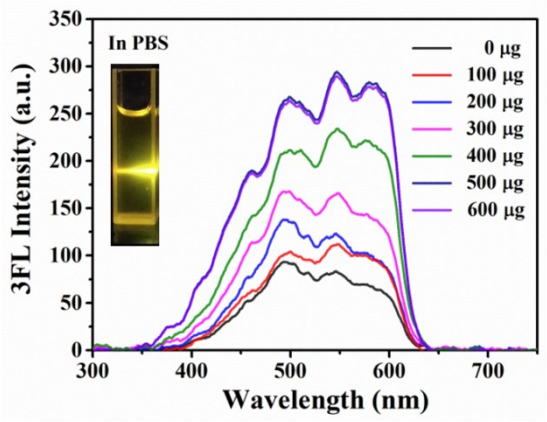

Figure. S28. Three-photon fluorescence spectra of **L3** in the presence of 0 ~ 600 μg liposomes (λ_{ex} = 1350 nm, c = 1 mM).

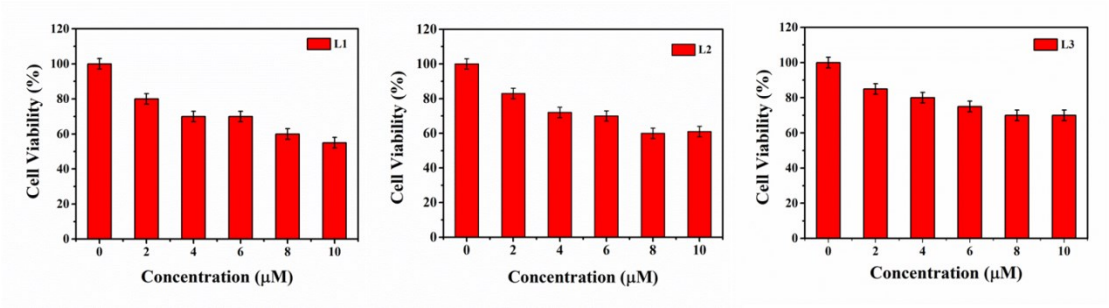

Figure. S29. Cell viability of HeLa cells treated by **L1**, **L2** and **L3** with different concentration (0，2, 4, 6, 8, 10 μM) for 24 h.

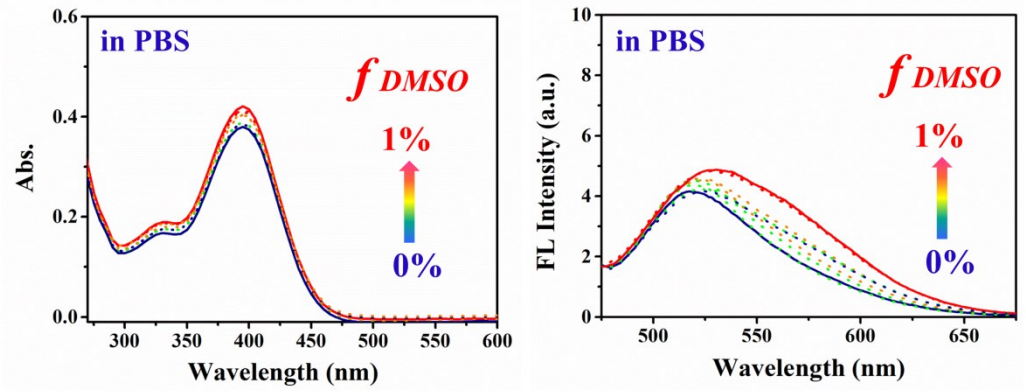

Figure. S30. The absorption/fluorescence spectra of **L3** (c = 0.01 mM) in PBS by adding different amounts of DMSO (0.1 - 1 %).

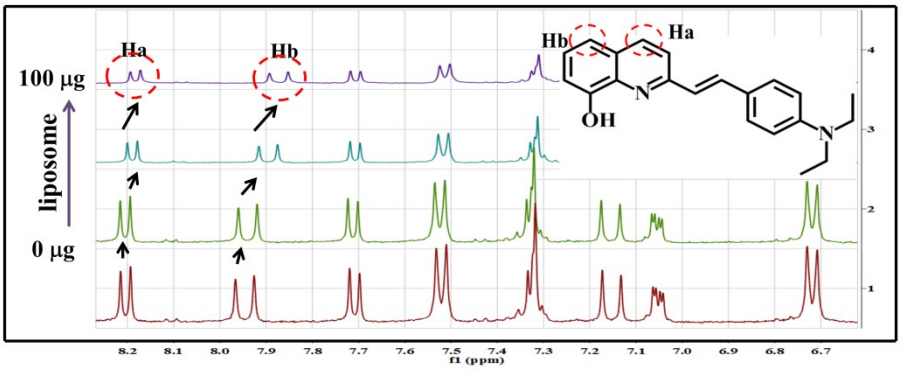

Figure. S31. Partial 1H NMR titration spectra for **L3** (1 mM) + liposome (0~100 μg) in DMSO-d_6/D_2O (v/v, 1 : 1).

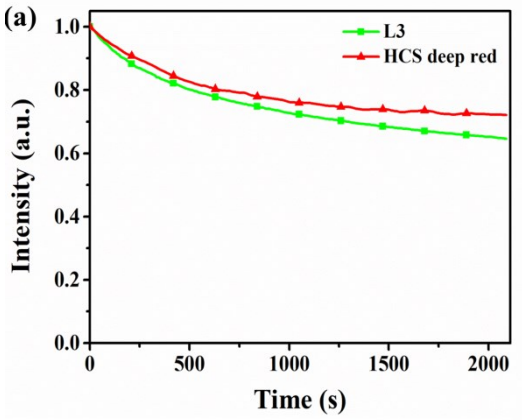

Figure. S32. Photostability of **L3** (λ_{ex} = 405nm) and commercial dye HCS Lipid TOXTM Deep Red (λ_{ex} = 633nm) in living HeLa cells.

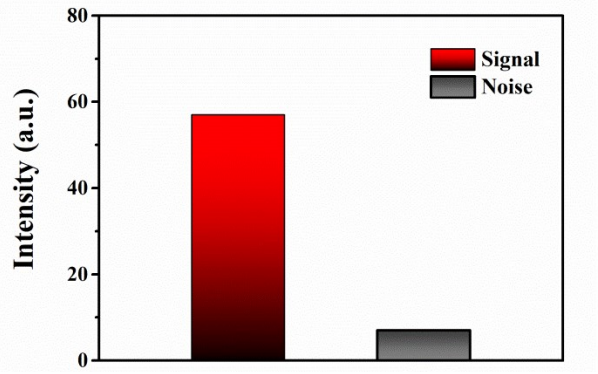

Figure. S33. The signal-to-noise ratio of confocal imaging.

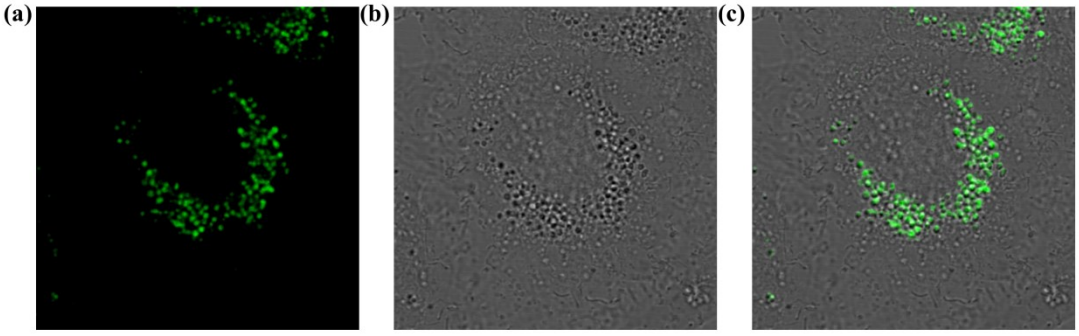

Figure. S34. (a) The two-photon fluorescence image of **L3** in living HeLa cells. (b) The bright-field image. (c) The merged image of a and b.

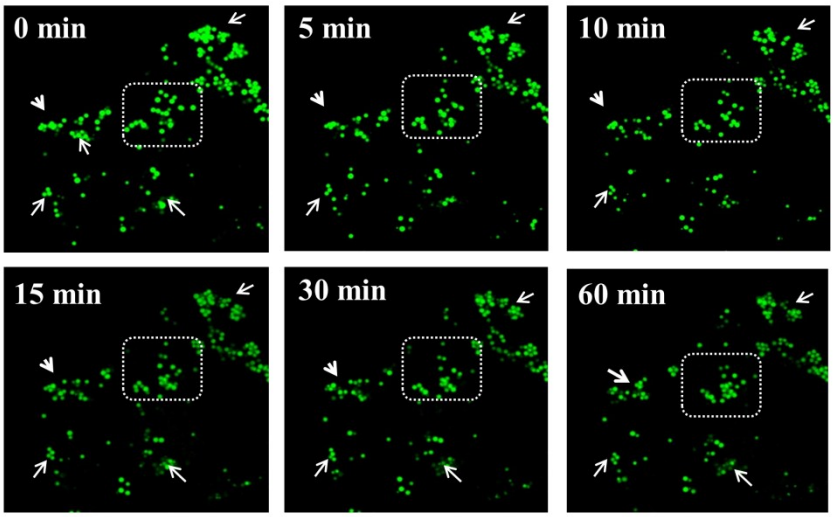

Figure. S35. Fluorescence images of tracking LDs movements Hela cells stained with **L3** (c = 10 μM, λ_{ex} = 438 nm).

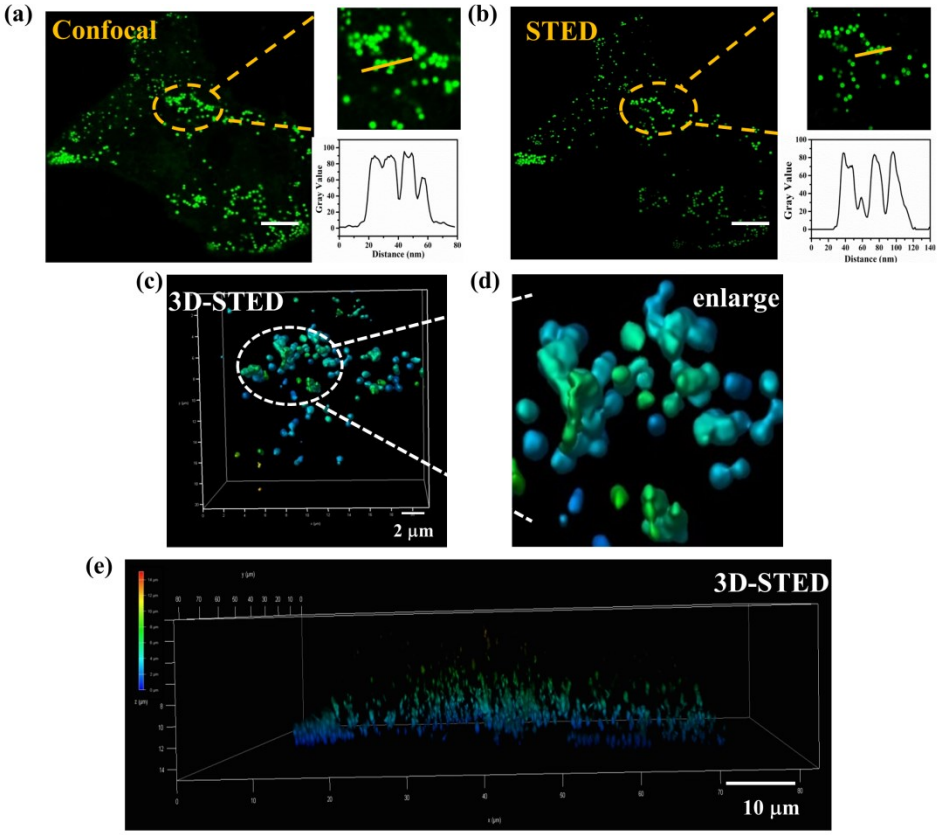

Figure S36. (a) Confocal fluorescence images of living HeLa cells incubated with 4 μM **L3** in DMSO/PBS (pH = 7.4, 1:99 v/v) for 10 min at 37 ºC (λ_{ex} = 405 nm, λ_{em} = 525 nm, scale bar = 10 μm); (b) The STED micrographs of L3 staining the Lipid droplets with a higher resolution using a 592 nm STED depletion laser (λ_{ex} = 405 nm, λ_{em} = 550–600 nm, scale bar = 10 μm); (c) Morphological characteristics of LDs stained with 4 μM **L3**, 3D-STED image; (d) The zoomin region from c; (e) 3D depth super-resolution imaging of lipid droplets.

Table S1. Crystal data collection and structure refinement of **L1, L2** and **L3**.

	L1	**L2**	**L3**
Empirical formula	$C_{17}H_{12}FNO$	$C_{19}H_{17}NO_3$	$C_{21}H_{22}N_2O$
Formula weight	265.28	307.34	318.41
T [K]	296	293	296
Crystal system	Monoclinic	Monoclinic	Triclinic
Space group	$P2_1/c$	C2/c	Pī
a [Å]	6.7867(11)	26.0843(10)	11.151(2)
b [Å]	14.848(2)	11.2427(3)	12.493(3)
c [Å]	13.118(2)	22.2883(8)	15.327(3)
α[°]	90	90	104.662(2)
β[°]	101.182(2)	101.990(3)	101.560(2)
γ[°]	90	90	114.181(2)

V/Å^3	1296.8(4)	6393.6(4)	1769.6(4)
Z	4	8	4
D calcd/(g cm^{-3})	1.359	1.347	1.197
F(000)	552	2729	682
Absorption coefficient/(mm^{-1})	0.095	0.849	0.074
Reflections collected	10018	19980	13901
GOF on F^2	1.017	1.053	1.044
R_1 [I >2σ(I)]	0.0389	0.0594	0.0566
wR_2 [I >2σ(I)]	0.092	0.1562	0.1580

Table S2. Selected bond lengths (Å) and angles (°) of **L1, L2** and **L3**.

L1			
F(5)-C(15)	1.363(17)	C(11)-C(12)	1.459(19)
O(1)-C(2)	1.363(16)	C(10)-C(11)	1.330(19)
N(1)-C(1)	1.365(16)	C(12)-C(13)	1.386(2)
N(1)-C(9)	1.331(16)	C(1)-C(6)	1.409(19)
C(9)-N(1)-C(1)	118.19(12)	C(10)-C(11)-C(12)	126.82(7)
C(7)-C(8)-C(9)	120.45(13)	C(9)-C(10)-C(11)	126.74(4)
O(1)-C(2)-C(3)	120.70(14)	F(1)-C(15)-C(14)	117.85(6)
L2			
O(5)-C(15)	1.366(5)	O(6)-C(23)	1.371(6)
O(2)-C(1)	1.190(7)	C(3)-N(1)	1.148(7)
C(6)-O(3)	1.374(5)	C(7)-O(3)	1.386(7)
C(19)-O(20)	1.319(6)	C(9)-C(10)	1.319(6)
C(1)-O(1)-C(29)	116.10(5)	C(2)-C(3)-N(1)	174.23(7)
C(6)-O(3)-C(7)	118.26(4)	C(9)-C(10)-C(11)	126.55(4)
C(15)-O(5)-C(16)	117.94(4)	C(23)-O(6)-C(24)	115.76(6)
L3			
O(5)-C(15)	1.366(5)	O(6)-C(23)	1.371(6)
O(2)-C(1)	1.190(7)	C(3)-N(1)	1.148(7)
C(6)-O(3)	1.374(5)	C(7)-O(3)	1.386(7)
C(19)-O(20)	1.319(6)	C(9)-C(10)	1.319(6)
C(1)-O(1)-C(29)	116.10(5)	C(2)-C(3)-N(1)	174.23(7)
C(6)-O(3)-C(7)	118.26(4)	C(9)-C(10)-C(11)	126.55(4)
C(15)-O(5)-C(16)	117.94(4)	C(23)-O(6)-C(24)	115.76(6)

Table S3. The Photophysical data of **L1, L2** and **L3** in different solvents.

Compounds	Solvent	λ_{max}^{abs} (nm)[a]	λ_{max}^{SPEF} (nm)[b]	Δν(nm)[c]	τ(ns)[d]	Φ[e]
L1	THF	343	438	95	--	--
	Acetonitrile	341	460	119	--	--
	DMSO	347	471	124	0.14	0.03
	H_2O	339	416	77	--	--
L2	THF	364	449	85	--	--
	Acetonitrile	359	462	103	--	--
	DMSO	370	474	104	0.17	0.07
	H_2O	354	461	107	--	--
L3	THF	403	510	107	--	--
	Acetonitrile	403	531	128	--	--
	DMSO	403	534	131	0.23	0.29
	H_2O	410	530	120	--	--

[a] Peak position of the longest absorption band.

[b] Peak position of 1PEF, excited at the absorption maximum.

[c]Stokes' shift in nm.

[d]Fluorescent lifetime.

[e]Quantum yields.

Table S4. Calculated linear absorption properties (nm), excitation energy (eV), oscillator strengths and major contribution for all the chromophores in DMSO.

Compounds	ΔE_1[a]	λ_{max}[nm][b]	Oscillator strengths	Nature of the transition
L1	4.38	347	0.6943	128(H)→129(L)(0.3750)
L2	3.96	372	0.6506	93(H)→94(L)(0.0584)
L3	3.65	405	0.6441	89(H)→90(L)(0.7864)

[a] The energy gap of the single-photon absorption band.

[b] Peak position of the maximum absorption band.

Table S5. The 2PA Cross-Section (GM, 1GM= 10^{-50} cm^4 s per photon) of **L1** ~ **L3** in DMSO with excitation wavelength around 700 ~ 960 nm, respectively (c = 1.0 × 10^{-3} mol/L).

Excitation Wavelength (nm)	**L1**	**L2**	**L3**
700	2.63	3.01	15.20

720	4.64	5.22	43.33
740	5.12	9.41	51.99
760	11.45	25.88	102.30
780	15.21	29.79	91.62
800	47.13	90.67	181.56
820	124.60	252.27	290.96
840	98.38	213.47	359.54
860	80.10	132.32	154.50
880	77.14	117.72	132.32
900	35.61	62.67	105.14
920	21.97	43.32	59.70
940	9.39	31.69	20.07
960	1.67	4.64	11.40

Table S6. The 3PA Cross-Section of **L3** in DMSO and PBS with excitation wavelength around 1150 ~ 1600 nm, respectively (c = 1.0 × 10^{-3} mol/L).

	Excitation Wavelength (nm)	**3PA Cross-Section (10^{-81}cm^{6}s^{2}photon^{-2})**
DMSO	1150	151.79
	1200	233.59
	1250	199.55
	1300	291.34
	1350	378.05
	1400	247.07
	1450	139.40
	1500	117.19
	1550	9.97
	1600	4.04
PBS	1150	7.55
	1200	9.26
	1250	9.07
	1300	13.02
	1350	14.88
	1400	14.09
	1450	10.92
	1500	10.01
	1550	6.81
	1600	1.01

Table S7. The 3PA Cross-Section (× 10^{-81}cm^{6}s^{2}photon^{-2}) of **L1** and **L2** in DMSO with excitation wavelength around 1150 ~ 1600 nm (c = 1.0 × 10^{-3} mol/L).

Excitation Wavelength (nm)	**L1**	**L2**
1150	8.14	5.62

1200	11.40	7.57
1250	9.84	6.45
1300	26.07	7.92
1350	18.40	6.71
1400	16.58	4.06
1450	11.78	3.35
1500	5.88	1.66
1550	5.30	1.53
1600	0.63	1.15

Table S8. The 3PA Cross-Section of **L3** when different volume of lipsome add with the excitation wavelength of 1350 nm.

	Excitation Wavelength (nm)	**3PA Cross-Section ($\times 10^{-81}$cm^{6}s^{2}photon^{-2})**
L3(in DMSO)	1350	378.05
L3(in PBS)	1350	14.02
L3 + 100μg liposome	1350	22.87
L3 + 200μg liposome	1350	27.50
L3 + 300μg liposome	1350	35.19
L3 + 400μg liposome	1350	43.10
L3 + 500μgliposome	1350	58.34
L3 + 600μg liposome	1350	55.95

References:

[1] Makarov, N. S.; Drobizhev, M.; Rebane, A., Two-photon absorption standards in the 550-1600 nm excitation wavelength range. *Opt. Express.* 2008, **16**, 4029-4047.

[2] S. V. Eliseeva, G. Aubock, F. V. Mourik, A. Cannizzo, B. Song, E. Deiters, A. S. Chauvin, M. Chergui and J. G. Bunzli, *J. Phys. Chem. B.*, 2010, **114**, 2932-2937.

[3] Z. H. Feng, D. D. Li, M. Z. Zhang, T. Shao, Y. Shen, X. H. Tian, Q. Zhang, S. L. Li, J. Y. Wu and Y. P. Tian, *Chem. Sci.,* 2019, **10**, 7228–7232.